Title: Fiber identification of braided composites using micro-computed tomography

Authors: Garrett W. Melenka*, Ali Gholami.

*Corresponding Author: gmelenka@yorku.ca

Abstract:

Braided composites contain interwoven fibers that are embedded in a matrix material. Advanced measurement methods are required to accurately measure and characterize braided composites due to their interwoven composition. Micro-computed tomography (μCT) is an X-ray based measurement method that allows for the internal structure of objects to be examined. High-resolution μCT of braided composites allows for their internal geometry to be accurately measured. Braid samples were measured with a voxel size of 1.0 μm^3, which resulted in a field of view of 4.904 x 4.904 x 3.064 mm^3. With this field of view, individual fibers within the braid yarns could be identified and measured. The scientific visualization software package Avizo and the XFiber extension was used to identify and measure braid yarn fibers from the collected μCT measurements. Fiber properties such as orientation angles (ϕ and θ), curved fiber length, tortuosity, and fiber diameter were obtained. Additionally, finite element mesh geometries of the braid yarns within a braided structure were created. The presented methodology provides a roadmap for the accurate modeling of braided composite unit cell geometries using high-resolution μCT data.

Keywords: Braided composites; micro-computed tomography; Fiber identification

1 Introduction

Braided composites consist of woven fibers embedded within a matrix [1]. Two dimensional (2D) braided composites are categorized into biaxial and triaxial configurations. Biaxial braided composites are produced using radial or Maypole braiders and consist of two yarns oriented at an angle ($\pm\theta$) from the longitudinal axial of the braid. In contrast, triaxial braids consist of additional longitudinal yarns [2]. Biaxial braided composites are commonly used due to their favorable mechanical properties and damage resistance over conventional laminated composites [3]. Since braids exhibit interwoven yarns, microstructural analysis is required.

Micro-computed tomography (μCT) is an X-ray based measurement method that can be used to assess the internal microstructure of an object [3,4]. The μCT method has been used to assess both biaxial and 3D braided composites [5,6]. In these studies, the overall 3D geometry of the braided composites was examined. The μCT has also been used to assess damage and failure of braided composites [7,8]. Geometry and porosity assessment of braided composites has been achieved using the μCT method [9–12]. In these studies, braid porosity has been evaluated by utilizing manual image segmentation and morphological operations to quantify fiber volume fraction, matrix volume fraction, and void volume fraction within braided composite structures. Additionally, the size and distribution of voids have been examined using the image segmentation method for braided composites. Current studies have focused on the overall structure of braided composites but have not been performed at high enough resolution to examine individual fibers within braid yarns [3].

Manual segmentation and analysis techniques are utilized to quantify structures from μCT data; however, manual methods are time-consuming, user-dependent and not as reproducible as other methods. For this reason, automated segmentation methods are required to improve the measurement and identification of structures from μCT data. The automated identification of filaments was implemented by Rigort *et al.* where they used this process to identify actin filament networks [13]. The work by Weber *et al.* performed automated tracing of microtubules in *C. elegans* embryos [14].

Short fiber composite materials have been characterized using an automated μCT segmentation process. Parameters of interest for short fiber composites are the orientation tensor for fibers dispersed within a matrix [15–17]. Fiber analysis using the μCT method has been performed for composites that exhibit randomly distributed short fibers by Karamov *et al.* [18]. In this work,

random glass fibers were examined within a polypropylene matrix. The glass fibers were examined for 3D fiber identification and structural tensor analysis. Two software packages were used for analysis, Avizo and VoxTex. Fiber-reinforced concrete was also examined by Ríos *et al*. [19]. Short and long steel fibers were added to concrete, and the orientation of fibers within the concrete was examined to examine the effect of fiber orientation on mechanical properties. Emerson *et al*. also used a fiber identification process to examine carbon fiber and glass fiber reinforced unidirectional laminates [20]. In this work, the authors note the challenges of using conventional image processing methods like Otsu's method for identifying individual fibers in images. Perciano *et al.* developed a custom fiber identification program, FibriPy, which uses Python and GPU based visualization to identify fibers from μCT data [21]. The μCT method and digital image correlations were used to automatically identify the orientation of short fibers within composite structures [22]. In another study, the software Volume Graphics was used to examine the ordination of 0/+45/-45/90 plies within a laminate [23]. These studies demonstrate that the μCT process can identify and measure individual fibers in composite structures.

Automated segmentation methods have been used with μCT to generate finite element analysis (FEA) models. Examples include the creating of an FEA model for non-crimp fabric composites [24]. The effect of short fiber orientation on mechanical properties was also investigated [25]. Micro-scale FEA models have also been generated based on synchrotron CT measurements of multi-directional carbon fiber composites [26]. Simulation of textile composites on the mesoscopic scale using μCT data has also been performed [27].

A geometrical model is required for performing analysis on braided composites. Geometrical models for braided composites have been developed; however, all models have assumptions that result in variations from physical samples [28–31]. As a result, an improved method for obtaining braid geometry is required.

In Melenka *et al.*, preliminary fiber analysis was performed using image segmentation techniques [11]. Previously, the void content and yarn geometry of natural fiber braided composites were examined using image segmentation techniques. It was noted that individual fibers could be visualized from the collected μCT scans; however, the fiber analysis was only performed on a single yarn tow and was a highly user-dependent process. It was also not possible to identify

individual fibers or perform statistical analysis on braid fibers using the manual segmentation process [11].

The method presented in this study will use an automated fiber tracing algorithm to identify and examine individual fibers within braided composite structures [13,14]. Scientific visualization software Avizo and the XFiber Extension will be used to automatically examine and identify individual fibers in braided composite samples measured using μCT image data. Braided composites typically utilize three scales for modeling and analysis: micro-scale (fibers and matrix), meso-scale (repeating braid unit cell), and macro-scale (braided structure) [32,33]. This work will provide accurate geometric data for the meso-scale modeling of braided composite structures. The geometry presented in this work can then be used to support the development of analytical or simulation-based models for braided composites.

2 Methods

2.1 Sample Preparation

Tubular braided composite preforms were produced using a Maypole braider (Steeger USA, K80–72, Steeger USA, Inman, SC). The braid samples were produced in a Regular (2/2) braid configuration using a 9.525 mm (3/8") mandrel. The braid yarns comprised of cellulose fibers (BioMid™, 1650 Denier, ENC International Inc, Burnaby, BC, Canada) embedded in a bio-based resin (SuperSap One, Entropy Resins, Bay City, MI). The braid yarns used in this study have a fiber denier of 1650 and consist of approximately 900 filaments with a filament diameter of 11μm. Two braid samples are examined in this work with nominal braid angles of 45° and 55º. The braid sample manufacturing details are summarized in Table 1.

Table 1: Braid sample geometry details

Manufacturing Parameter	**Sample (1)**	**Sample (2)**
Nominal Braid Angle (º)	45	55
Nominal Inner Diameter (mm)	9.525	9.525
Number of braid yarns	36	36
Braiding Pattern	Regular (2/2)	Regular (2/2)

2.2 Micro-computed tomography of Braided Samples

Braid samples were examined using a desktop µCT (SkyScan 1272 microtomograph, Bruker-MicroCT, Kontich, Belgium) with a voxel size of 1.0 μm^3 to examine individual fibers within the braided structure. The braid samples were imaged using an X-ray voltage of 40 kV and with a current of 200 µA. Image noise for the µCT was reduced by using a frame averaging value of 2 with a rotation step of 0.2°. Nine hundred (900) projections were collected for each sample. Due to the resolution and field of view chosen in this work, only a partial section of each braid sample was visualized. The resultant images produced a partial section of each braid for analysis.

The radiographs of the braid images were converted to cross-sectional images using reconstruction software (NRECON 1.7.1.0, Bruker, Belgium). Reconstructed cross-sectional images were created with 8-bit bitmap (BMP) format. Both braid sample image datasets were 4904 x 4904 x 3064 pixels or 4.904 x 4.904 x 3.064 mm. Cross-sectional images of the two braid samples are shown in Figure 1. The sample field of view can be seen in this figure. Additionally, fiber tows, matrix, individual fibers and voids are identified in this image. In addition, 3D volume views of the two braid samples are shown in Figure 1 (c) and (d).

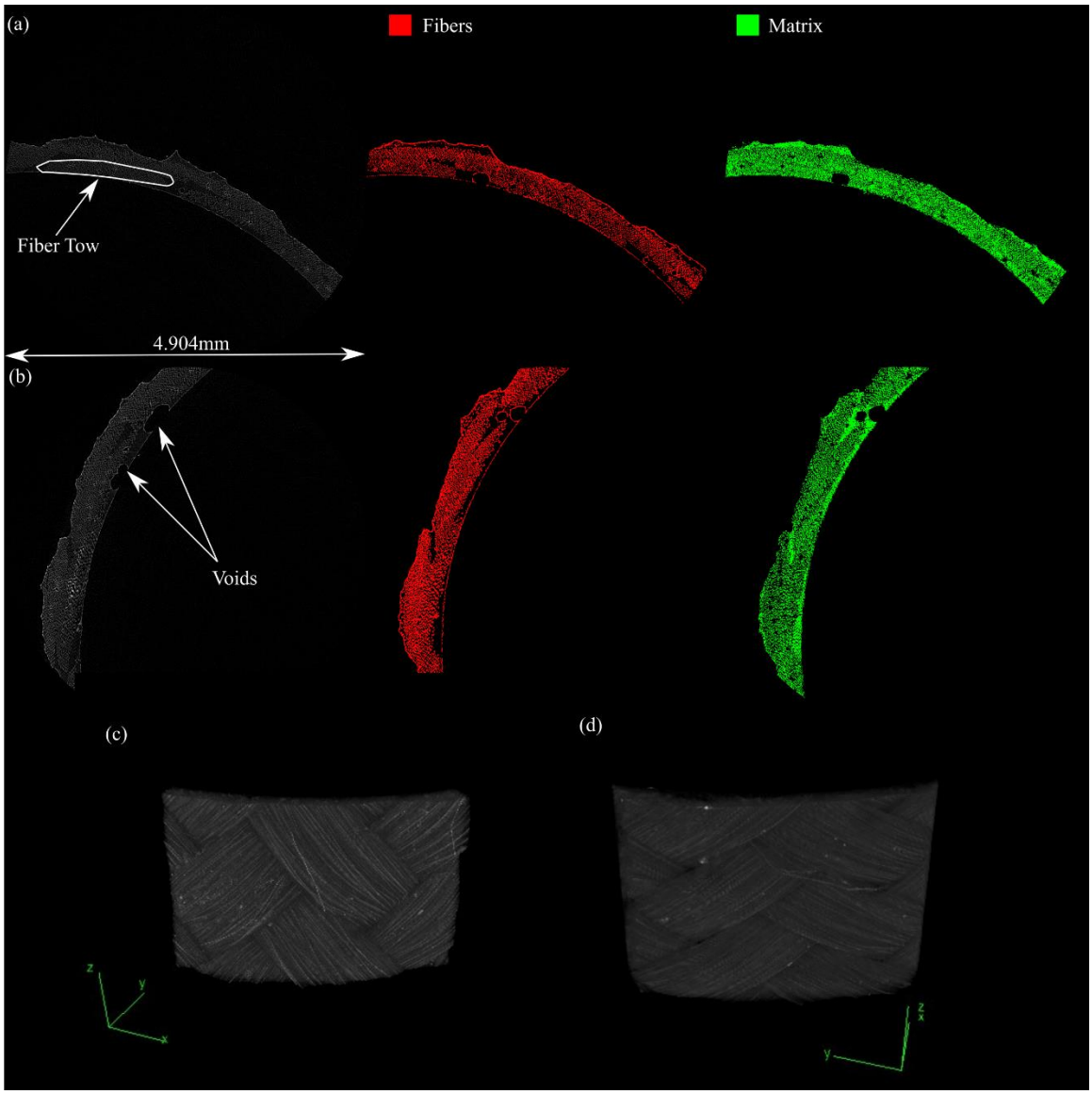

Figure 1: Example of cross-sectional images of braid samples created through µCT imaging. Fiber Tows, matrix, individual fibers and voids are identified (a) Sample (1) braid example cross-section (b) Sample (2) braid example cross-section (c) 3D volume view of Sample (1) (d) 3D volume view of Sample (2)

2.3 Braid Yarn Identification and Characterization

Examination of fibers within braided composite samples was performed using a commercial scientific visualization software package (Avizo 2019.3, Thermo Fisher Scientific, Waltham, Massachusetts, USA). The XFiber Extension was utilized for fiber identification. The XFiber module requires an NVIDIA graphics card with CUDA (Compute Unified Device Architecture) 1.3 or higher. The workstation used for this analysis comprised of a processor (i9-9940X CPU 14-core/28 thread processor at 3.0 GHz, Intel, Santa Clara, California, USA), 128 gigabytes of RAM

(4x32GB DDR4 Vengeance, Corsair, Fremont, California, USA) and graphics card (NVIDIA GeForce GTX 1660 6GB 1408 CUDA cores, Gigabyte, New Taipei City, Taiwan).

The initial dataset collected from the μCT consisted of images with a size of 4904 x 4904 x 3064 pixels or 4.904 x 4.904 x 3.064 mm^3 with a voxel size of 1.0 mm^3. The dataset was down-sampled to a size of 613x613x383 pixels for fiber analysis to allow for the rapid analysis of the μCT image datasets. The XFiber Extension used two modules for analysis: 'Cylinder Correlation' and 'Trace Correlation Lines'. The analysis settings for the 'Cylinder Correlation' and 'Trace Correlation Lines' modules are summarized in Table 2. Results generated from XFiber analysis were exported into MATLAB format (MATLAB R2020a, The MathWorks, Natick, MA, USA) for visualization and further data processing. The parameters detailed in Table 2 are used to identify solid or hollow cylinders in an image dataset using a normalized cross-correlation algorithm [13,14]. The user defines initial parameters to allow for the identification of cylinders in a dataset. 'Angular sampling' determines the angular frequency that a half-sphere is sampled. 'Minimum continuation quality' determines the minimum value to continue a line. Larger values favor earlier termination of lines. 'Search Cone Length' determines the maximum step size between two points on a line.

Table 2: Fiber identification parameters using the XFiber extension of Avizo for analysis of braided composite samples

Analysis Parameter	**Sample (1)**	**Sample (2)**
Cylinder Length (mm)	0.3	0.3
Angular Sampling (º)	5	5
Cylinder Mask Radius (μm)	10	10
Outer Cylinder Radius (μm)	6	6
Minimum Seed Correlation	68	68
Minimum Continuation Quality	115	115
Direction Coefficient	0.3	0.3
Search Cone Length (mm)	0.5	0.5
Search Cone Angle (º)	37	37
Minimum Step Size	10	10

3 Results and Discussion

Using the XFiber extension, fibers are identified using a cross-correlation algorithm and uses a search cone for fiber tracing [13,14]. The resulting identified fibers using the XFiber analysis process are shown in Figure 2. After individual fibers are identified, a fiber tracing algorithm is utilized. A comparison of braid yarn geometries created using a conventional image segmentation process

and using the fiber identification process are also shown in Figure 2. Figure 2 (a) and (b) show a close-up image of a cross-section of the braid sample where individual fibers can be seen. Figure 2 (b) braid images created from the binarized and thresholded images using the process described by Melenka *et al.* [11]. The braid fibers were identified by thresholding the μCT images using a grayscale range of 30-255 to separate the braid fibers from the epoxy matrix. The challenge with the binarization method for identifying fibers is that multiple fibers connect, which presents significant difficulty separating the fibers from each other.

In the images shown in Figure 2 (a) and (b) and geometries shown in Figure 2 (c) and (d), it is not possible to distinguish individual yarns; however, the total fiber volume fraction can be calculated using this method. Figure 2 (c) and (d) also shows that fiber identification using a binarization method allows for the total fiber volume to be found, but individual fibers are not distinguishable. Figure 2 (e) and (f) show braid samples with individual fibers identified. The braid images shown in Figure 2 (e) and (f) demonstrate that the cross-correlation algorithm used by the XFiber algorithm is better suited to identifying individual fibers within the braid unit cells.

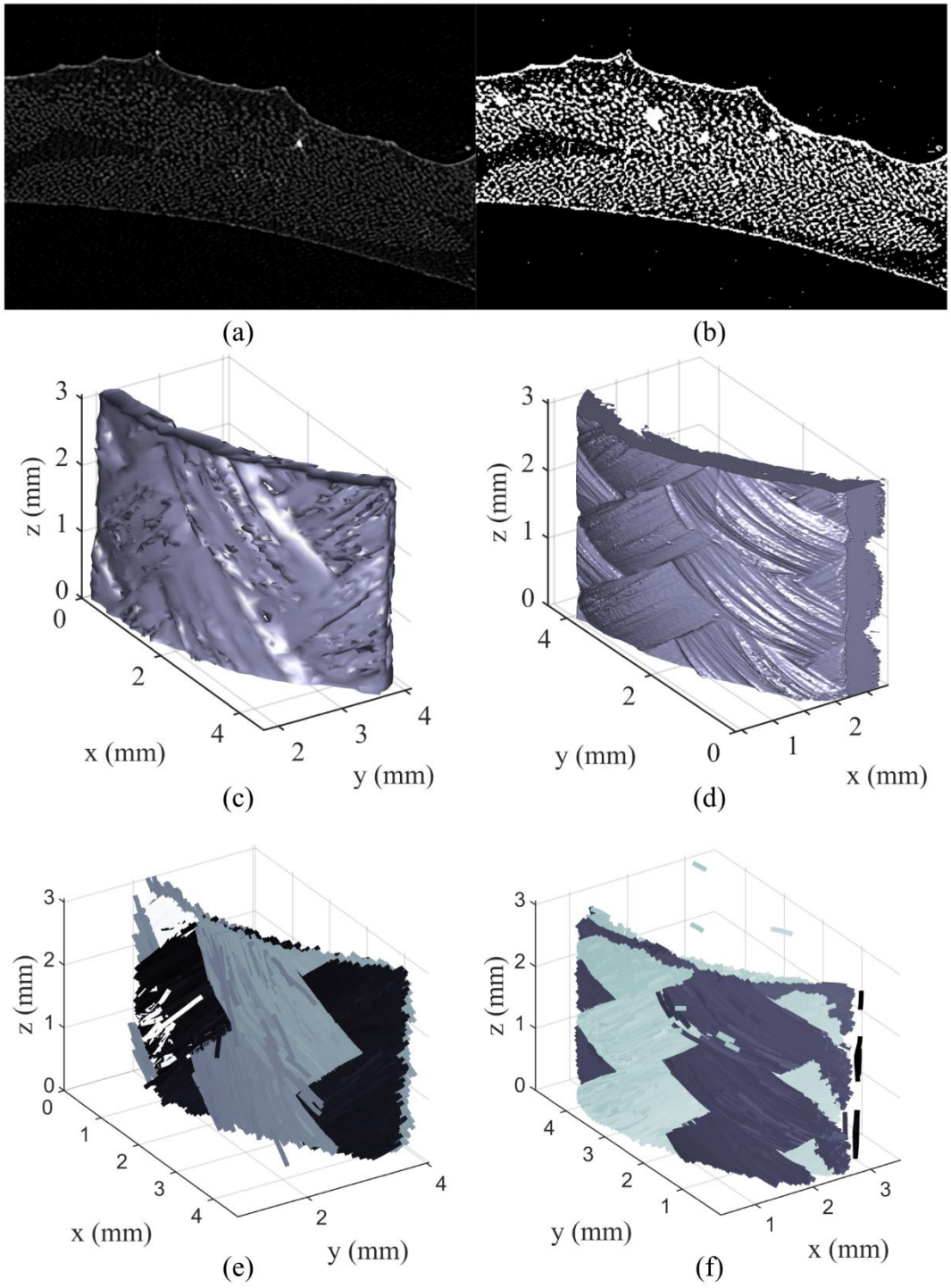

Figure 2: Identification and analysis of braid fibers using μCT data (a) Close-up image of braid cross-section showing individual fibers (b) binarized image of braid cross-section (c) Volume rendering of braid sample- Sample (1) (d) Volume rendering of braid-Sample (2) (e) Individual fibers identified -Sample (1). (f) Individual yarns identified- Sample (2))

In addition to identifying the individual fibers of the two braid samples, as shown in Figure 2, detailed information regarding each fiber can be obtained. Data extracted from each fiber includes curved fiber length, fiber chord length, orientation angles (ϕ and θ), fiber diameter, fiber cross-sectional area and tortuosity.

The resulting measured fiber orientation angles θ and ϕ for the two braid samples are visualized in Figure 3. The orientation angles are defined using the coordinates shown in Figure 3 (a). The orientation angle θ represents the angle formed from the z-axis of the sample and ranges from 0 to 90 degrees. The orientation angle ϕ is measured from *x*-axis to the *y*-axis in the *xy*-plane and ranges from 0 to 360 degrees. Since the braid samples examined in this work were oriented with their longitudinal axis coincident with the *z*-axis of the μCT machine, the orientation angle θ obtained for each fiber corresponds to the braid angle of the samples. The orientation angle ϕ corresponds to the undulation of the braid yarns. The fiber orientation angles are also used to represent the orientation of short fibers within composites [15–19].

Figure 3 (b) and (c) shows the fiber orientation angle ϕ and Figure 3 (d) and (e) show the fiber orientation angle θ. The orientation angle ϕ show that two predominant angles exist for both Samples (1) and (2). Additionally, the fiber orientation angles θ shown in Figure 3 (c) and (d) show that the braid fibers predominately feature a single angle measured from the sample *z*-axis.

Once the individual fibers have been identified, it is possible to examine features such as Tortuosity (T), fiber orientation angles (θ and ϕ), fiber diameter and the curved fiber length. Fiber tortuosity, *T*, is defined in Equation (1), where *C* is the curved fiber length, and *L* is the fiber chord length. The results from the braid fiber analysis for the two braid samples are summarized in Table 3. In this table, the average and standard deviation for each braid fiber measurement are reported.

$$T = \frac{C}{L} \qquad (1)$$

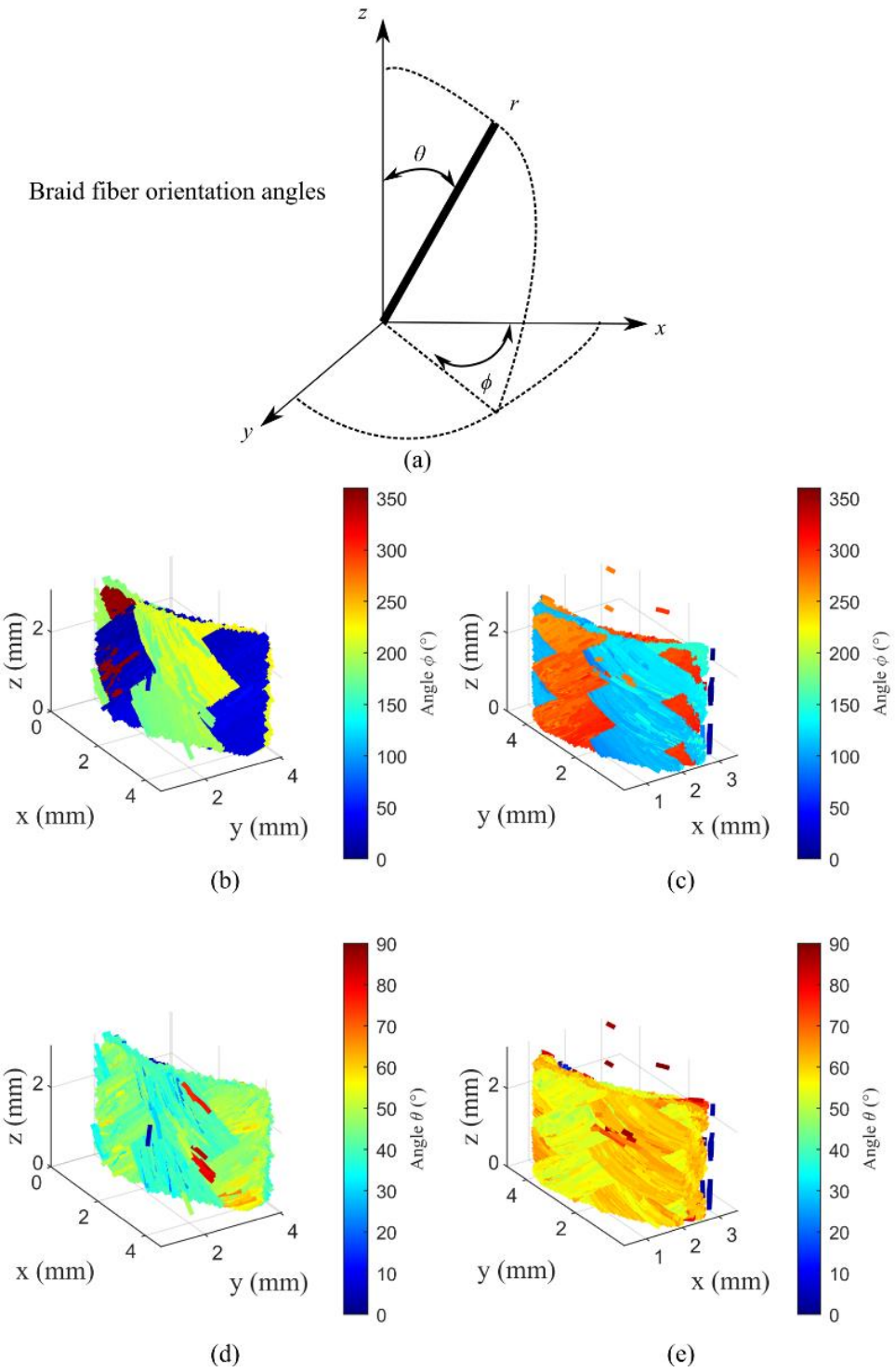

Figure 3: Braid sample orientation angle visualization for individual yarns (a) Braid fiber orientation angles (b) Orientation angle ϕ for sample (1) (c) Orientation angle ϕ for sample (2) (d) Orientation angle θ for sample (1) (e) orientation angle θ for sample (2)

Table 3: Braid fiber analysis summary

	Sample (1)	**Sample (2)**
Fiber Orientation Angle ϕ_1 (º)	205.04	113.82
Fiber Orientation Angle ϕ_2 (º)	27.17	285.94
Fiber Orientation Angle θ (º)	41.88 ± 9.41	58.29 ± 9.24
Fiber Curved Length (mm)	1.65 ± 1.04	1.58 ± 1.31
Fiber Tortuosity (mm/mm)	1.01 ± 0.01	1.01 ± 0.02
Fiber Diameter (μm)	19.06 ± 11.43	17.92 ±7.37

The average fiber orientation angle for Sample (1) was 41.88±9.41º, and for Sample (2) 58.29±9.24º. The fiber orientation angle θ shown in Figure 3corresponds to the braiding angle of the two samples reported in Table 1. Since, in both cases, the yarn orientation is measured relative to the longitudinal axis of the braid samples, the fiber orientation angle θ corresponds to the braid angle of the samples. Deviations from the nominal braid angle reported in Table 1 result in fiber orientation variations that occur during the braid manufacturing and epoxy impregnation process.

The average fiber diameter found for Sample (1) was 19.06±11.43 μm, and the average fiber diameter for Sample (2) was 17.92±7.37 μm. For both braid samples examined in this work, the obtained fiber diameter values represent an overestimation of the reported fiber diameter for the braid yarns. The reported fiber diameter for the fiber yarns used in this study was 11 μm. The overestimation of the braid fiber diameter may be due to reducing the resolution of the initial μCT dataset size from 4904 x 4904 x 3064 to 613x613x383. The down-sample step may have reduced the fidelity of the image data resulting in an overestimation of the yarn fiber diameter. Additionally, the scan resolution used in this work with a voxel size of 1.0 μm^3 may not have been sufficient to resolve individual fibers fully. A higher resolution scan using a voxel size of less than 1.0 μm^3 may be necessary for more accurate fiber diameter measurement using the process outlined in this study.

Avizo and the XFiber module allowed for the automated identification of fibers within two braided composite samples. The method outlined in this work is advantageous over conventional image processing and segmentation methods that require custom algorithms to measure and identify features in μCT images. In addition, data can be obtained to describe the 3D geometry of braid fibers, as summarized in Table 3 and Figure 3. A significant drawback of the Avizo processing

method is that substantial memory, processing power, and graphics card memory is required. For this reason, image down-sampling or the use of sub-volumes may be necessary to perform analysis.

Finally, finite element analysis (FEA) meshes of the two braid samples were generated using Avizo and the XFiber module. The FEA meshes of the two samples are shown in Figure 4. The FEA meshes shown in Figure 4 can subsequently be used for the simulation of braid samples. The FEA analysis of the two braid samples is out of the scope of this work since yarn properties, boundary conditions, loading conditions, and simulation of the epoxy matrix must be considered. Simulations for braided composites commonly use a unit cell geometry where the unit cell is a small repeating unit used to represent the braid structure. Unit cell geometries have been considered for FEA analysis of braided composites; however, in these models, braid yarns are considered to be solid, and individual fibers are not considered [34,35].

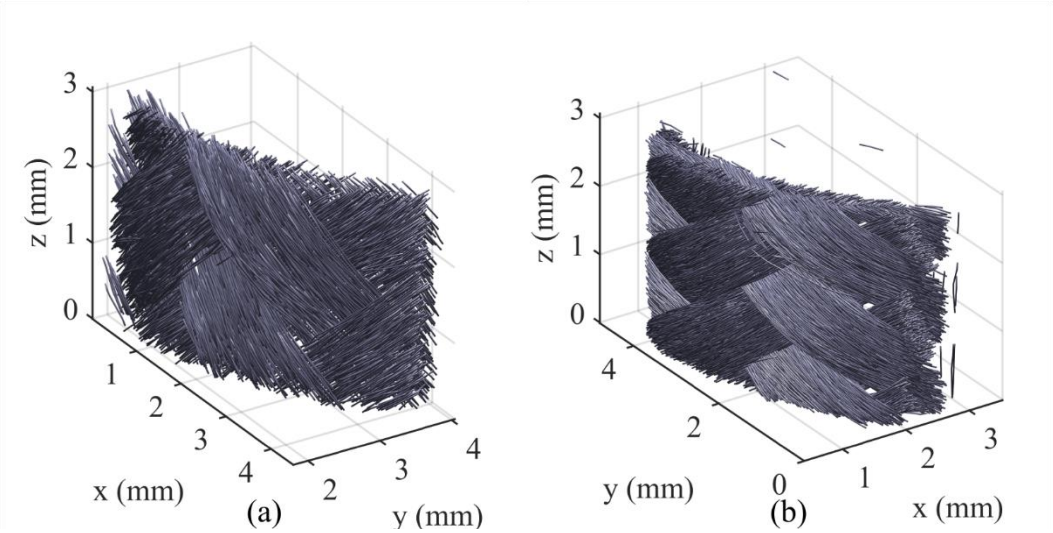

Figure 4: Creation of finite element analysis meshes of braids samples from fiber path data (a) Sample (1) (b) Sample (2)

4 Conclusions

In this study, two braided composite samples were examined using the μCT measurement method. The braid samples were scanned using an image voxel size of 1.0 μm^3, which resulted in a field of view of 4.904 x 4.904 x 3.064 mm^3. A section of braid samples was examined at this resolution so that individual braid yarn fibers could be resolved and measured.

Using the scientific visualization software package Avizo and the XFiber Extension, it was possible to identify and characterize individual fibers from the collected μCT image data of the two braid samples. The fiber identification process allows for measuring fiber orientation angles (ϕ and θ), curved fiber length, fiber diameter, and tortuosity. Also, accurate 3D geometries of the braid fibers can be generated for further analysis using numerical simulation software.

The results presented in this work provide a methodology for automatically analyzing braided composite structures using the μCT technique. The results presented in this work can then support numerical models for braided composites that accurately represent their fibrous nature.

5 Conflict of Interest

The author declares no conflicts of interest with respect to the research, authorship or publication of this article.

6 Data Availability Statement

The raw/processed data required to reproduce these findings cannot be shared at this time as the data also forms part of an ongoing study.

7 Acknowledgments

The author would like to acknowledge the Natural Sciences and Engineering Research Council (NSERC) Canada RGPIN- 2018-05899. CMC Microsystems provided the software used in this study.

8 References

1. Ayranci, C., Fahim, A. & Munro, M. A novel strain sensor for reinforced concrete structures. *Strain* **44**, 191–200 (2008).
2. Ko, F. K. Braiding. *ASM Int. Eng. Mater. Handbook.* **21**, 69–77 (2001).
3. Melenka, G. W. & Ayranci, C. Advanced measurement techniques for braided composite structures: A review of current and upcoming trends. *J. Compos. Mater.* 002199832090310 (2020) doi:10.1177/0021998320903105.
4. Stock, S. R. X-ray microtomography of materials. *Int. Mater. Rev.* **44**, 141–164 (1999).
5. Melenka, G. W., Lepp, E., Cheung, B. K. O. & Carey, J. P. Micro-computed tomography analysis of tubular braided composites. *Compos. Struct.* **131**, 384–396 (2015).
6. Ya, J., Liu, Z. & Wang, Y. Micro-CT Characterization on the Meso-Structure of Three-Dimensional Full Five-Directional Braided Composite. *Appl. Compos. Mater.* **24**, 593–610 (2017).
7. Li, Y., Sun, B. & Gu, B. Impact shear damage characterizations of 3D braided composite

with X-ray micro-computed tomography and numerical methodologies. *Compos. Struct.* **176**, 43–54 (2017).

8. Zhou, H. *et al.* Micro-XCT analysis of damage mechanisms in 3D circular braided composite tubes under transverse impact. *Compos. Sci. Technol.* **155**, 91–99 (2018).

9. Melenka, G. W., Lepp, E., Cheung, B. K. & Carey, J. P. Micro-computed tomography analysis of tubular braided composites. *Compos. Struct.* **131**, 384–396 (2015).

10. Bruni-bossio, B. M., Melenka, G. W., Ayranci, C. & Carey, J. P. Micro-computed tomography analysis of natural fiber and bio-matrix tubular-braided composites. (2019) doi:10.1177/0021998319853023.

11. Melenka, G. W., Bruni-Bossio, B. M., Ayranci, C. & Carey, J. P. Examination of voids and geometry of bio-based braided composite structures. *IOP Conf. Ser. Mater. Sci. Eng.* **406**, 012012 (2018).

12. Unlusoy, C. & Melenka, G. W. Flexural testing of cellulose fiber braided composites using three dimensional digital image correlation. *Compos. Struct.* **230**, 111538 (2019).

13. Rigort, A. *et al.* Automated segmentation of electron tomograms for a quantitative description of actin filament networks. *J. Struct. Biol.* **177**, 135–144 (2012).

14. Weber, B. *et al.* Automated tracing of microtubules in electron tomograms of plastic embedded samples of Caenorhabditis elegans embryos. *J. Struct. Biol.* **178**, 129–138 (2012).

15. Weissenböck, J. *et al.* Comparative Visualization of Orientation Tensors in Fiber - Reinforced Polymers. 1–9 (2018).

16. de Pascalis, F. & Nacucchi, M. Relationship between the anisotropy tensor calculated through global and object measurements in high-resolution X-ray tomography on cellular and composite materials. *J. Microsc.* **273**, 65–80 (2019).

17. Advani, S. G. & Tucker, C. L. The Use of Tensors to Describe and Predict Fiber Orientation in Short Fiber Composites. *J. Rheol. (N. Y. N. Y).* **31**, 751–784 (1987).

18. Karamov, R. *et al.* Micro-CT based structure tensor analysis of fibre orientation in random fibre composites versus high-fidelity fibre identification methods. *Compos. Struct.* **235**, 111818 (2020).

19. Ríos, J. D., Leiva, C., Ariza, M. P., Seitl, S. & Cifuentes, H. Analysis of the tensile fracture properties of ultra-high-strength fiber-reinforced concrete with different types of steel fibers by X-ray tomography. *Mater. Des.* **165**, 107582 (2019).

20. Emerson, M. J., Jespersen, K. M., Dahl, A. B., Conradsen, K. & Mikkelsen, L. P. Individual fibre segmentation from 3D X-ray computed tomography for characterising the fibre orientation in unidirectional composite materials. *Compos. Part A Appl. Sci. Manuf.* **97**, 83–92 (2017).

21. Perciano, T., Ushizima, D., Krishnan, H., Parkinson, D. & Sethian, J. FibriPy: A software environment for fiber analysis from 3D micro-computed tomography data. *Adv. Mater.* -

TechConnect Briefs 2017 **1**, 25–28 (2017).

22. Bernasconi, A., Carboni, M. & Ribani, R. On the combined use of Digital Image Correlation and Micro Computed Tomography to measure fibre orientation in short fibre reinforced polymers. *Compos. Sci. Technol.* **195**, 108182 (2020).

23. Sietins, J. M., Sun, J. C. & Jr, D. B. K. Fiber orientation quantification utilizing X-ray micro-computed tomography. *J. Compos. Mater.* **55**, 1109–1118 (2021).

24. Auenhammer, R. M., Mikkelsen, L. P., Asp, L. E. & Blinzler, B. J. Automated X-ray computer tomography segmentation method for finite element analysis of non-crimp fabric reinforced composites. *Compos. Struct.* **256**, 113136 (2021).

25. Lionetto, F. *et al.* Correlation between elastic properties and morphology in short fiber composites by X-ray computed micro-tomography. *Compos. Part A Appl. Sci. Manuf.* **140**, 106169 (2021).

26. Sencu, R. M. *et al.* Generation of micro-scale finite element models from synchrotron X-ray CT images for multidirectional carbon fibre reinforced composites. *Compos. Part A Appl. Sci. Manuf.* **91**, 85–95 (2016).

27. Badel, P., Vidal-Sallé, E., Maire, E. & Boisse, P. Simulation and tomography analysis of textile composite reinforcement deformation at the mesoscopic scale. *Compos. Sci. Technol.* **68**, 2433–2440 (2008).

28. Alpyildiz, T. 3D geometrical modelling of tubular braids. *Text. Res. J.* **82**, 443–453 (2012).

29. Wang, Y. *et al.* A new geometric modelling approach for 3D braided tubular composites base on Free Form Deformation. *Compos. Struct.* **136**, 75–85 (2016).

30. Ning, F., Potluri, P., Yu, W. & Hearle, J. Geometrical modeling of tubular braided structures using generalized rose curve. *Text. Res. J.* **87**, 474–486 (2017).

31. Rawal, A., Gupta, S., Saraswat, H. & Sibal, A. Geometrical modeling of near-net shape braided preforms. *Text. Res. J.* **85**, 1055–1064 (2015).

32. Byun, J.-H. The analytical characterization of 2-D braided textile composites. *Compos. Sci. Technol.* **60**, 705–716 (2000).

33. Melenka, G. W., Pastore, C. M., Ko, F. K. & Carey, J. P. Advances in 2-D and 3-D braided composite material modeling. in *Handbook of Advances in Braided Composite Materials: Theory, Production, Testing and Applications* 321–363 (2016). doi:10.1016/B978-0-08-100369-5.00009-X.

34. Ji, X. *et al.* Multi-scale simulation and finite-element-assisted computation of elastic properties of braided textile reinforced composites. *J. Compos. Mater.* **48**, 931–949 (2014).

35. Xu, L., Kim, S. J., Ong, C. H. & Ha, S. K. Prediction of material properties of biaxial and triaxial braided textile composites. *J. Compos. Mater.* **46**, 2255–2270 (2012).